

Supporting Information

Solution processed N-trialkylatedtriindoles for Organic Field Effect Transistors

C.Ruiz,^a I. Arrechea-Marcos, A. Benito-Hernández,^a E.Gutierrez-Puebla,^a A. Monge-Bravo,^aJ. T. López
Navarrete, M. C. Ruiz Delgado, R. Ponce Ortiz and Berta Gómez-Lor*^a

*E-mail: bgl@icmm.csic.es

Contents	Page
1 Electronic Properties of compounds 2-4	S2
2 DFT theoretical eigenvectors for the experimental Raman bands	S4
3 Molecular structure of 2-4 determined by single crystal analysis	S5
4 Powder X-ray diffractograms of aggregates of 2-4	S6
5 Differential Scanning Calorimetry of 2-4	S8
6 AFM images of solution processed films of 2-4	S10
7 GIXRD spectrum of solution-processed thin films of 4 on OTS-treated substrates	S11
8 Explanation to Checkcif Alerts of 3 and 4	S12

1. Electronic Properties of compounds 2-4

Absorption spectra. UV-vis studies were carried out on a PerkinElmer Lambda XLS+ spectrometer. Fluorescence spectra were recorded on an Aminco SLM 8000 spectrophotometer.

Cyclic Voltammetry Measurements. Cyclic voltammetry (CV) experiments were performed on a Bioanalytical Systems Inc. (BASi) Epsilon electrochemical workstation in a three-electrode cell at room temperature under a nitrogen atmosphere. Electrochemical measurements were carried out in acetonitrile solution ($c = 1 \times 10^{-3}$ M) containing 0.1 M tetra-n-butylammonium hexafluorophosphate (TBAPF₆) of supporting electrolyte at a scan rate 100 mV/s. A three electrode setup was used including a platinum working electrode, a Ag/AgCl (3 M NaCl) reference electrode, and a platinum wire auxiliary electrode. Ferrocene was used as an internal standard, and all potentials were referenced to the ferrocene/ferrocenium redox couple.

2-4 derivatives present nearly identical absorption spectra and cyclic voltammograms. From the first oxidation process we can estimate a HOMO level -5,08 eV and from the optical gap we estimate an HOMO-LUMO gap of 3,36 eV which render a LUMO level of -1,72 eV. The value of the HOMO and LUMO energy levels of these compounds are adequate for the use as p-type semiconductors in organic electronic devices.

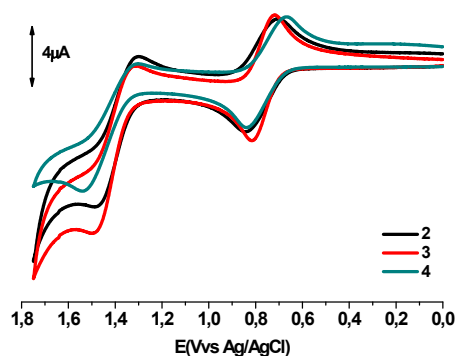


Figure S1. Cyclic voltammograms of **2-4** at $c = 1 \times 10^{-3}$ molL⁻¹ recorded in CH₂Cl₂/ 0.1M tetra-n-butylammonium hexafluorophosphate (TBAPF₆) measured versus Ag/AgCl (3M NaCl) and containing ferrocene as internal standard. Measurements were performed at a scan rate 100mV/s using a Pt working electrode and a Pt wire auxiliary electrode.

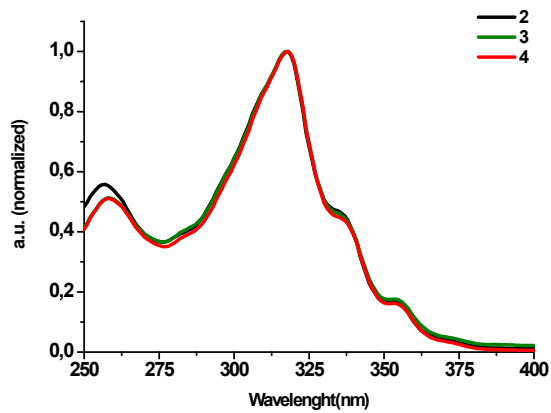


Figure S2. Experimental UV-Vis spectra of **2-4** at $c = 1 \times 10^{-6} \text{ molL}^{-1}$ recorded in CH_2Cl_2 .

2. DFT theoretical eigenvectors for the experimental Raman bands

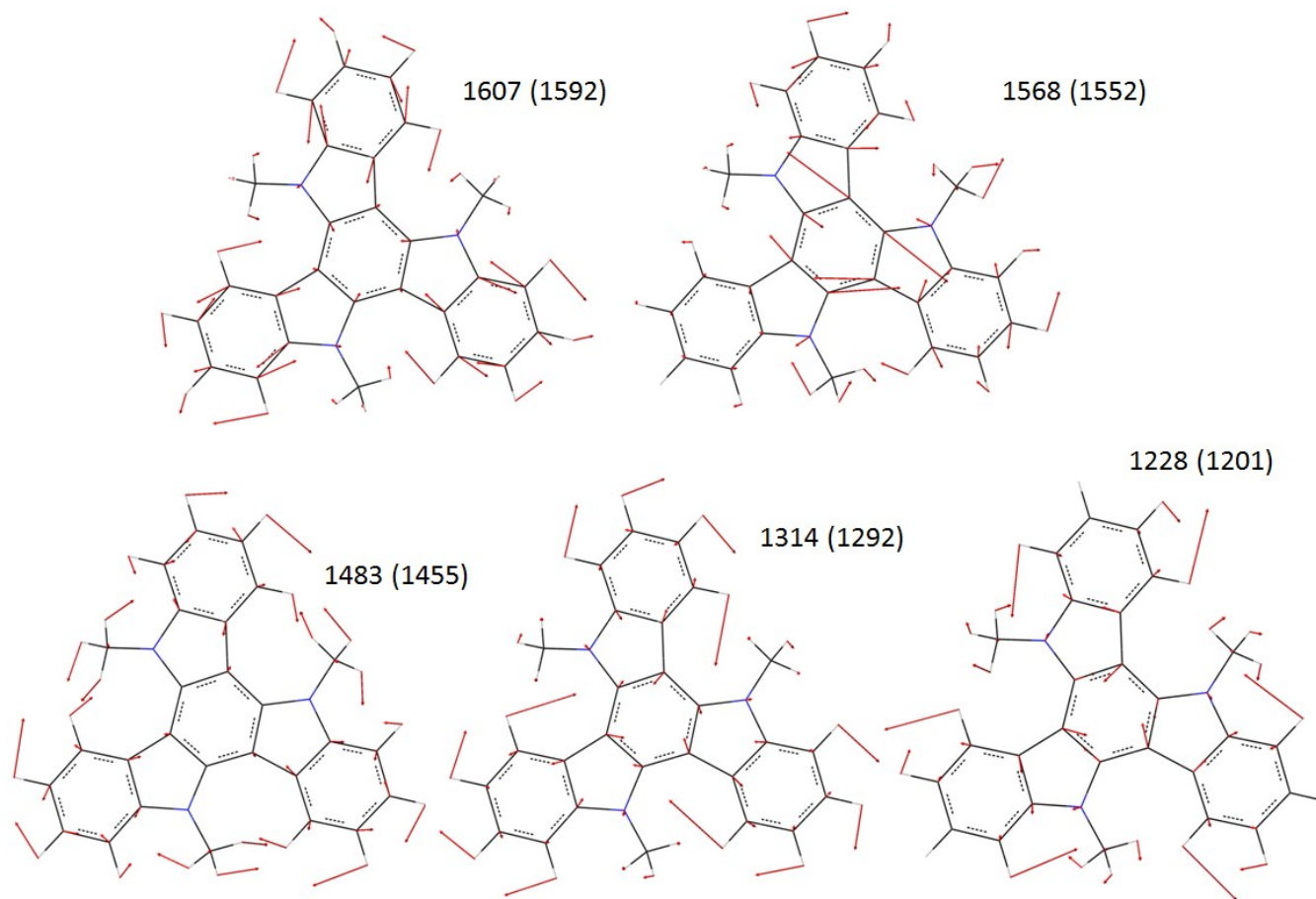


Figure S3: B3LYP/6-31G** selected eigenvectors for the discussed experimental Raman bands. The experimental and theoretical values (within parenthesis) are shown in cm^{-1} .

3. Molecular structure of 2-4 determined by single crystal analysis.

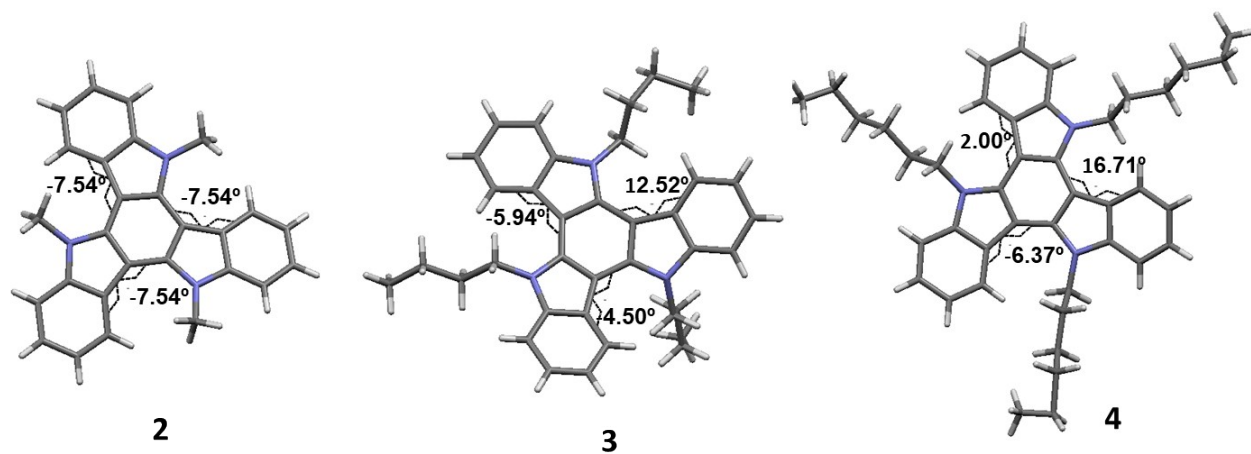


Figure S4 Molecular structure of compounds 2-4 showing the dihedral angles between the central and peripheral rings of the triindole platform.

4. Powder X-ray diffractograms of aggregates of 2-4.

X-ray powder diffractograms were recorded in a Bruker D8 diffractometer with a Sol-X energy dispersive detector, working at 40 kV and 30 mA and employing $\text{CuK}\alpha$ ($\lambda = 1.5418 \text{ \AA}$) filtered radiation. The diffractograms were registered with a step size of 0.02° and exposure time of 0.5 s per step and a 2θ range of $5\text{-}30^\circ$.

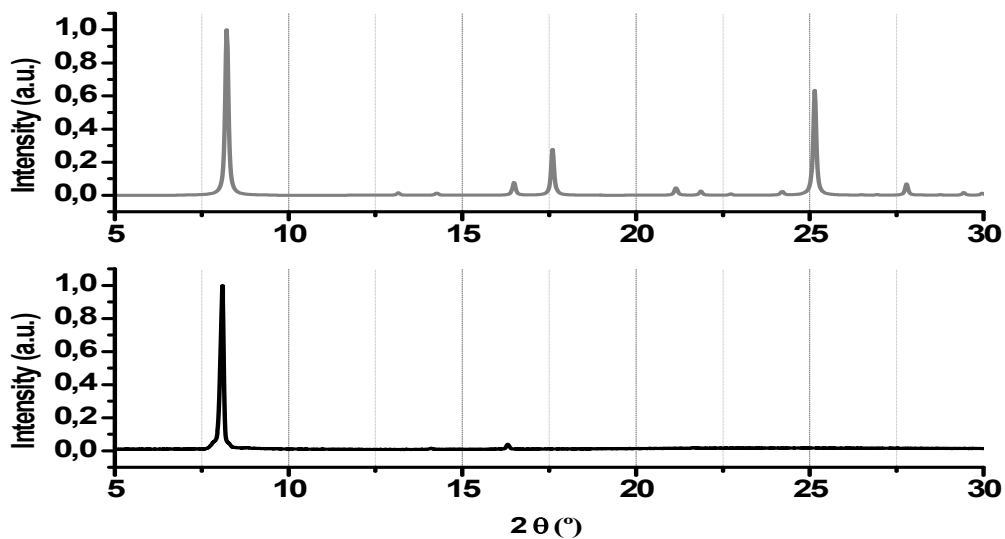


Figure S5. Powder X-ray diffractograms obtained from the single crystal data (above) and the experimental Powder X-ray diffractograms of the aggregates of **2** deposited by drop-casting on the substrate (below).

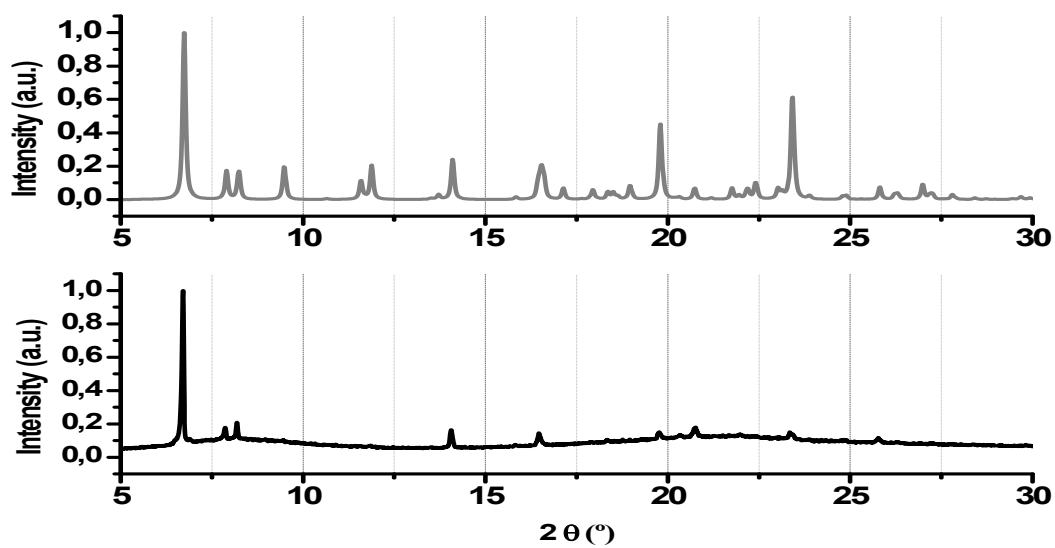


Figure S6. Powder X-ray diffractograms obtained from the single crystal data (above) and the experimental Powder X-ray diffractograms of the aggregates of **3** deposited by drop-casting on the substrate (below).

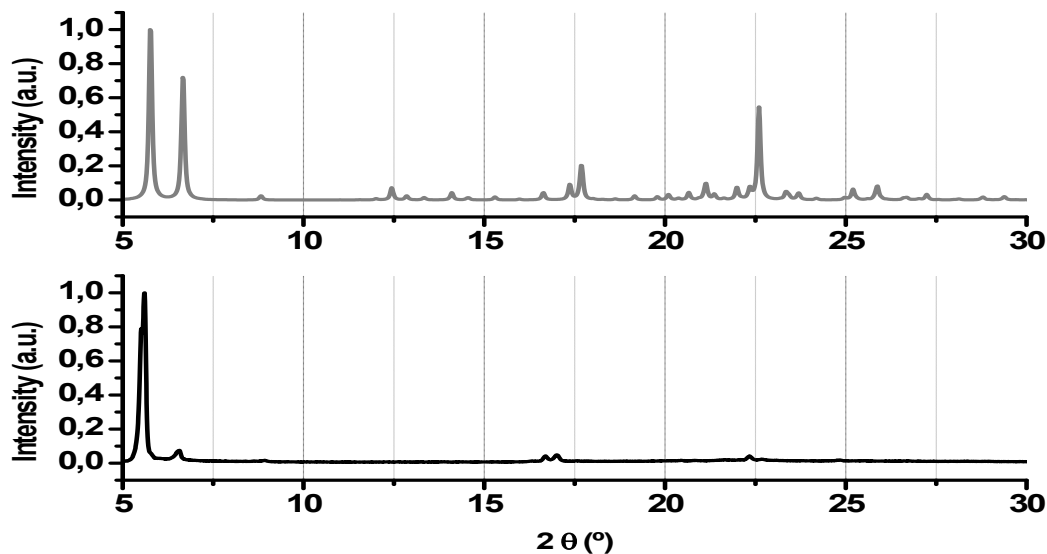
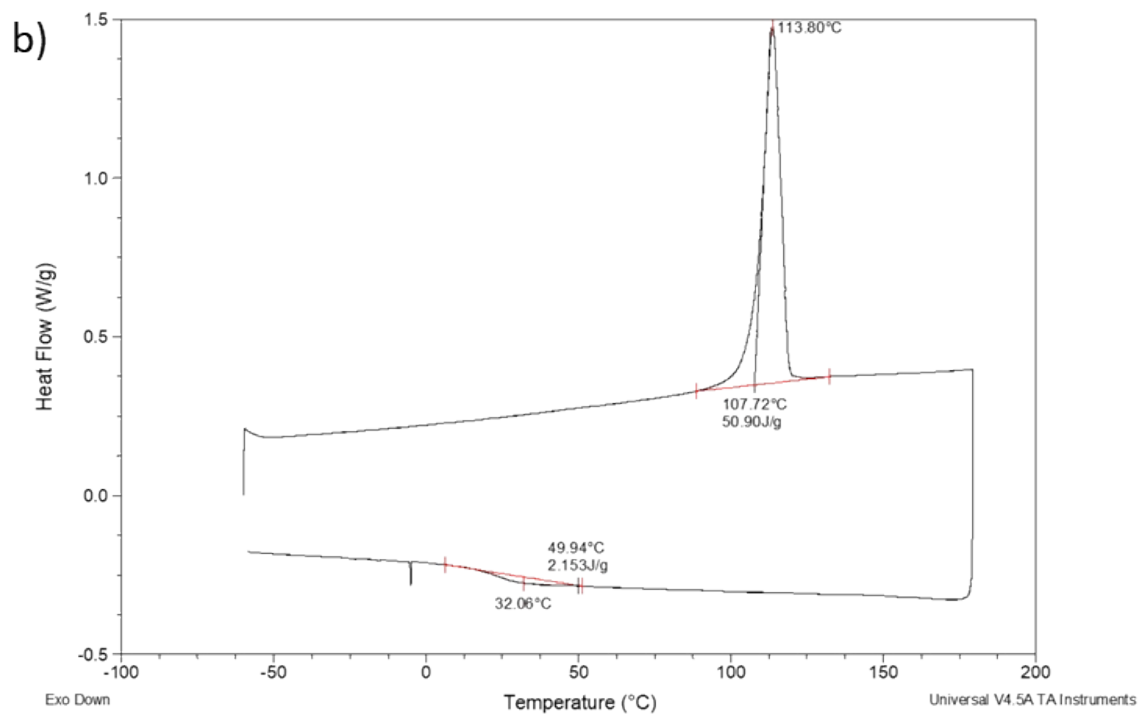
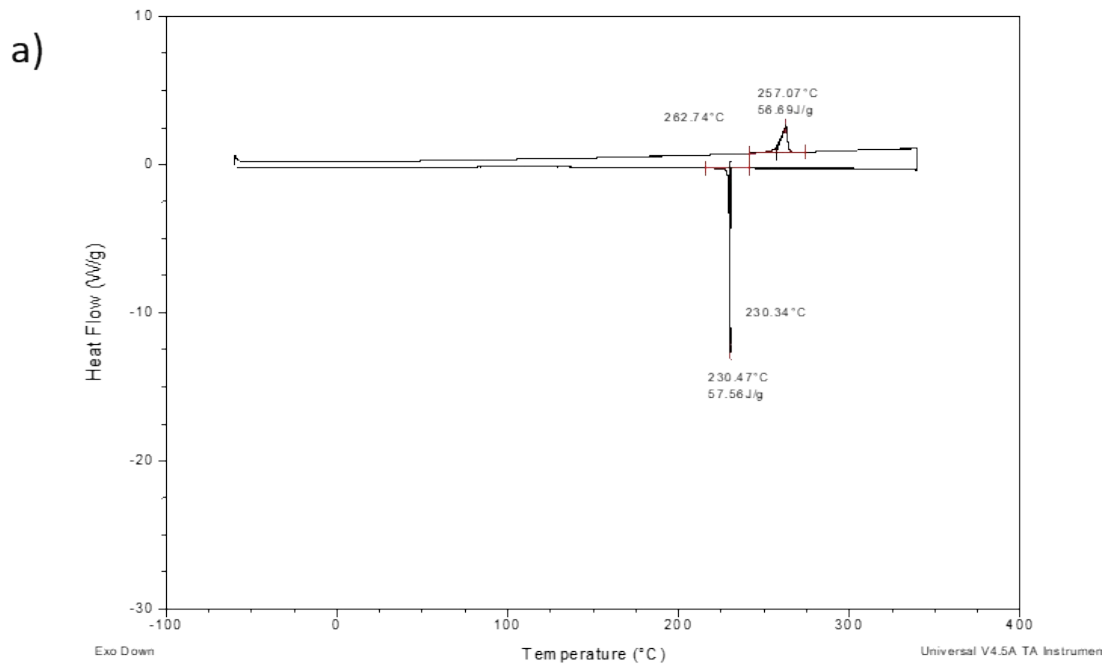


Figure S7. Powder X-ray diffractograms obtained from the single crystal data (above) and the experimental Powder X-ray diffractograms of the aggregates of **4** deposited by drop-casting on the substrate (below).

5. Differential Scanning Calorimetry of 2-4

The transition temperatures and enthalpies were measured by differential scanning calorimetry with a TA Instrument Discovery DSC calorimeter operated under N₂ at a scanning rate of 10 °C min⁻¹ on both heating and cooling. The apparatus was calibrated with indium (156.6 °C; 28.71 Jg⁻¹) as a standard.



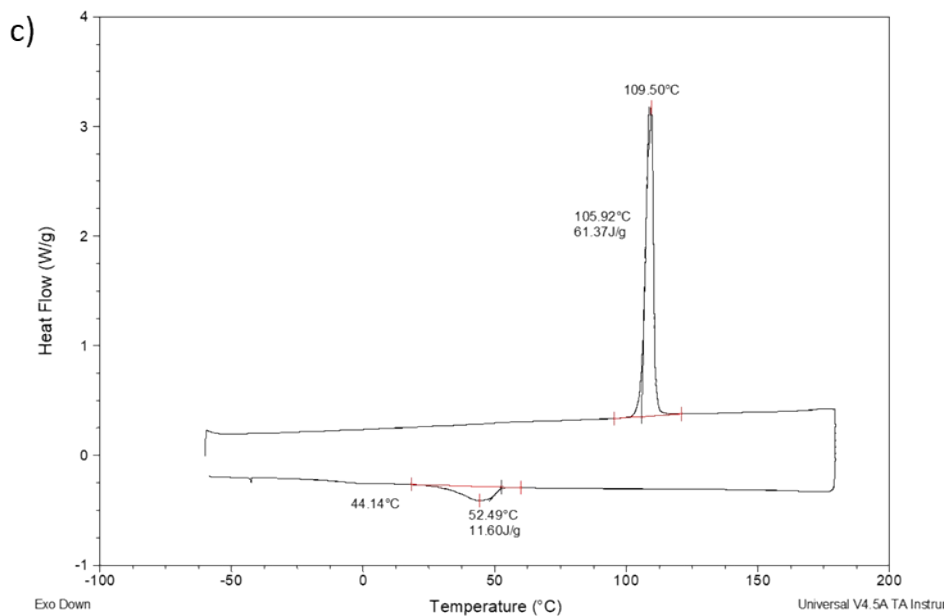


Figure S8. Differential Scanning calorimetry (DSC) traces of first heating/cooling cycles of (a) **2**, (b) **3**, (c) **4**.

6. AFM images of solution processed films of 2-4.

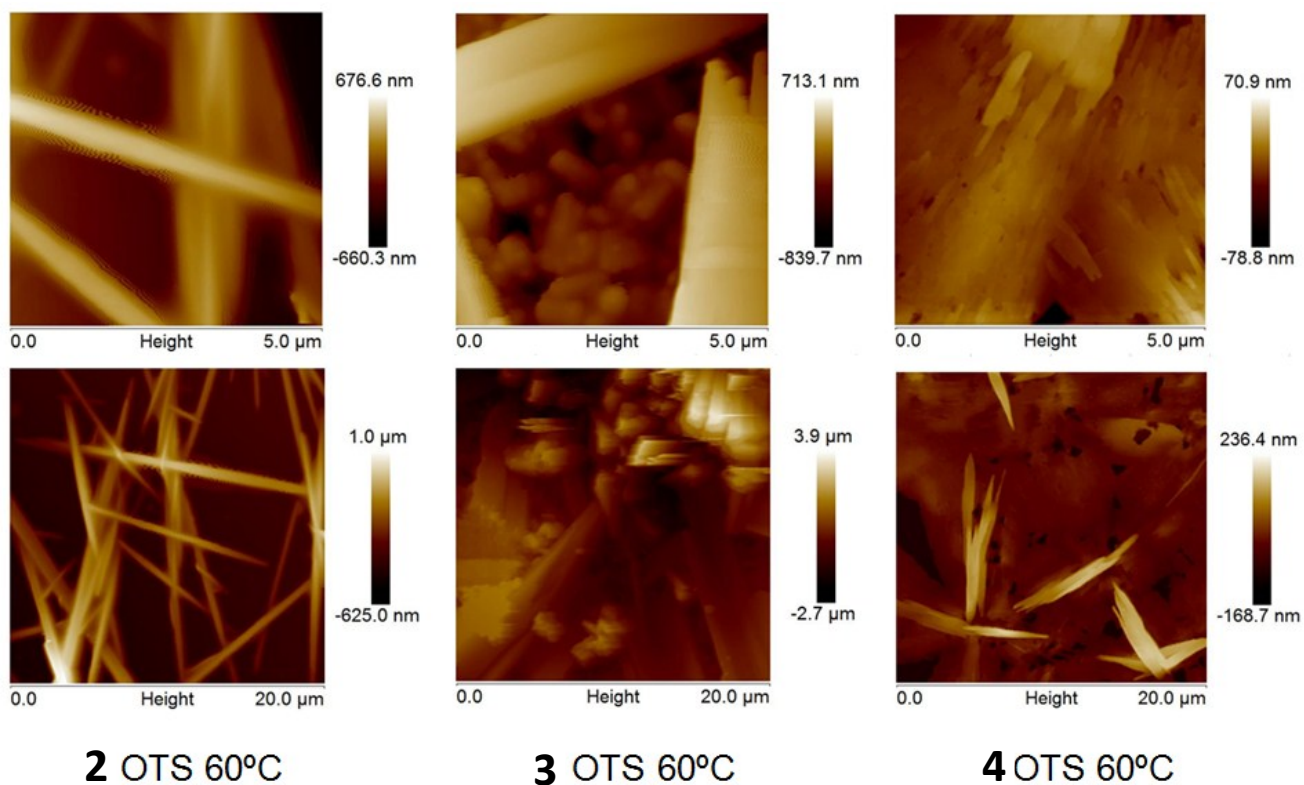


Figure S9. Tapping mode AFM images ($5\ \mu\text{m} \times 5\ \mu\text{m}$, top and $20\ \mu\text{m} \times 20\ \mu\text{m}$, bottom) of solution processed films of **2-4** on OTS-functionalized substrates and annealed at the indicated temperatures. OTS: octadecyltrichlorosilane.

7. GIXRD spectrum of solution-processed thin films of 4 on OTS-treated substrates.

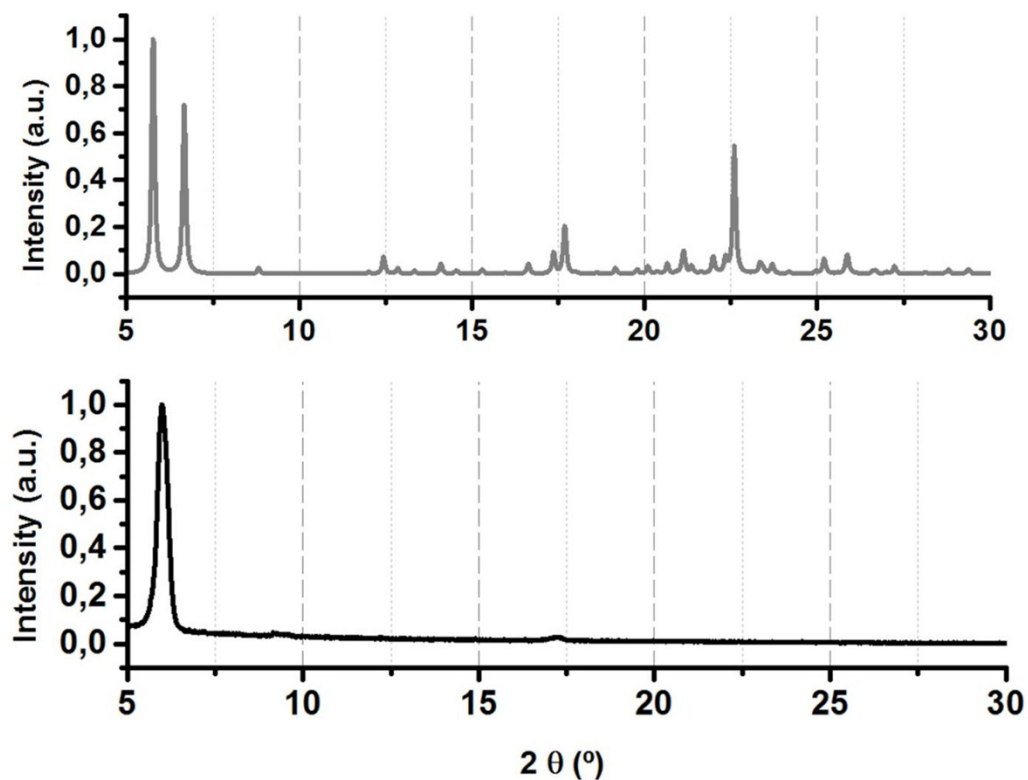


Figure S8. Normalized powder X-ray diffractogram obtained from the single crystal data (above) and GIXRD spectrum of solution-processed **4** thin films on OTS-treated substrates and annealed at 60°C.

8. Explanation to checkcif Alerts of 3 and 4

Thermal disorder, especially on the last carbon of the butyl and hexyl chains makes that both crystals diffract poorly at high angles. Several crystals were checked, collecting the best ones of each compound.

Checkcif_3

PLAT029_ALERT_3_A _diffn_measured_fraction_theta_full Low 0.896 Note

The butyl chains are very affected of thermal motion, especially the chain (C33-C34-C35-C36, approximately perpendicular to the molecule). This fact provokes that crystals of **2c** diffracts poorly at high angles, resulting several high angle reflections with negative intensities (543). These reflections were omitted during the integration process to get a satisfactory convergence during the refinement.

PLAT230_ALERT_2_B Hirshfeld Test Diff for C34 -- C35 .. 7.8 s.u.

The high thermal disorder observed on the chain causes this alert in spite that DELU restriction was used. Some electronic density residual peaks appear around the atoms C34 and C35, but none satisfactory model of positional disorder could be modeled.

PLAT911_ALERT_3_B Missing # FCF Refl Between THmin & STh/L= 0.600 543 Report. This alert comes from the same motives than ALERT A.

Checkcif_4

THETM01_ALERT_3_B The value of $\sin(\theta_{\max})/\text{wavelength}$ is less than 0.575

The Calculated $\sin(\theta_{\max})/\text{wavelength} = 0.5706$, in the accepted limit.

PLAT230_ALERT_2_B Hirshfeld Test Diff for C34 -- C35 .. 10.6 s.u.

PLAT230_ALERT_2_B Hirshfeld Test Diff for C41 -- C42 .. 8.1 s.u.

PLAT410_ALERT_2_B Short Intra H...H Contact H14 .. H31B .. 1.86 Ang.

The high thermal disorder observed on the hexyl chains causes these alerts in spite that DELU restriction was used in both cases (C34-C35, and C41-C42).